

On the Conformational Memory in the Photodissociation of Formic Acid

E. Martínez-Núñez,^{*,†} S. A. Vázquez,[†] I. Borges, Jr.,[‡] A. B. Rocha,[§] C. M. Estévez,^{||}
J. F. Castillo,[⊥] and F. J. Aoiz[⊥]

Departamento de Química Física, Universidade de Santiago de Compostela, 15782, Santiago de Compostela, Spain, Departamento de Química, Instituto Militar de Engenharia, Rio de Janeiro 22290-270, Brazil, Instituto de Química, Departamento de Físico-Química, Universidade Federal do Rio de Janeiro, Rio de Janeiro 21949-900, Brazil, Departamento de Química Física, Universidade de Vigo, 36200 Vigo, Spain, and Departamento de Química Física, Facultad de Química, Universidad Complutense de Madrid, Spain

Received: January 10, 2005; In Final Form: January 31, 2005

The photodissociation of formic acid at 248 and 193 nm was investigated by classical trajectory and RRKM calculations using an interpolated potential energy surface, iteratively constructed using the B3LYP/aug-cc-pVDZ level of calculation. Several sampling schemes in the ground electronic state were employed to explore the possibility of conformational memory in formic acid. The CO/CO₂ branching ratios obtained from trajectories initiated at the cis and at the trans conformers are almost identical to each other and in very good accordance with the RRKM results. In addition, when a specific initial excitation that simulates more rigorously the internal conversion process is used, the calculated branching ratio does not vary with respect to those obtained from cis and trans initializations. This result is at odds with the idea of conformational memory in the ground state proposed recently for the interpretation of the experimental results. It was also found that the calculated CO vibrational distributions after dissociation of the parent molecule at 248 nm are in agreement with the experimental available data.

Introduction

It was recently suggested that the CO + H₂O and CO₂ + H₂ eliminations in the photodissociation of formic acid (FA) proceed under geometrical memory and dynamical control.^{1–3} In other words, that the geometry of the transient species formed in the S₁→S₀ decay determines the product branching ratio. Absorption of a photon of 248 nm (115 kcal/mol) excites FA to the S₁ electronic state. At this wavelength, dissociation on the S₁ surface, intersystem crossing (ISC), or funneling through S₀/S₁ conical intersections (CI) to the ground state are all energetically inaccessible.³ Therefore, apart from fluorescence, the system may relax back to the ground state via vibronic interaction between the vibrational manifold of the S₀ and S₁ states and dissociate through one of the above channels. In the gas phase, the CO + H₂O elimination is clearly preferred over formation of CO₂ and H₂. This observation, and the fact that ab initio calculations predict virtually the same barrier for both channels, led Su et al.¹ to state the above suggestion.

Upon photoexcitation of FA at 193 nm (~148 kcal/mol) in the gas phase, elimination of CO and CO₂ also occurs after internal conversion (IC) to the ground state, but direct dissociation on the S₁ surface to give HCO + OH is the dominant channel. However, in an Ar matrix environment, Khriachtchev et al.² did not observe any isolated OH radicals, which suggests either a small cage-exit probability at this excitation energy (both radicals could rapidly recombine to FA) or a negligible

branching ratio for this channel in solid Ar.² They found a CO/CO₂ ratio of ~0.4 for the photolysis of *cis*-FA and ~5 for *trans*-FA. These results led them to propose a mechanism in the ground state (after IC) in which the elimination occurs faster than the randomization of the torsion coordinate mixing the conformers, thus following the previous suggestion by Su et al.¹

Apparently, the model of conformational memory in the ground electronic state faces with the fact that the barrier for cis–trans isomerization (13 kcal/mol) is markedly lower than the barriers for CO + H₂O and CO₂ + H₂ eliminations (~70 kcal/mol). To investigate this issue in more detail, we carried out ab initio and dynamics (RRKM and trajectory) calculations for the photodissociation of formic acid at 248 and 193 nm.

Computational Details

A. Ab Initio Calculations. Ab initio and density functional calculations (DFT) were first performed to explore the ground state potential energy surface of the molecule. Specifically, geometry optimizations were carried out with the hybrid functional B3LYP and with the quadratic configuration interaction (QCI) method with single and double excitations (QCISD), using the aug-cc-pVDZ and the aug-cc-pVTZ basis sets, respectively. The QCISD energies were subsequently refined by adding a triples contribution to the energy [QCISD(T)]. All the stationary structures were characterized as minima or transition states by frequency calculations and, to ensure that the transition structures are the correct species connecting reactants with products, intrinsic reaction coordinate calculations for all the channels were done at the B3LYP/aug-cc-pVDZ level of theory.

* Corresponding author. E-mail: qfemilio@usc.es

[†] Universidade de Santiago de Compostela.

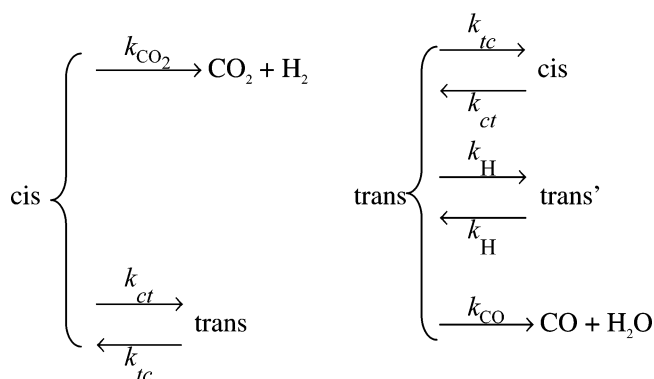
[‡] Instituto Militar de Engenharia.

[§] Universidade Federal do Rio de Janeiro.

^{||} Universidade de Vigo.

[⊥] Universidad Complutense de Madrid.

B. Kinetic and RRKM Calculations. The microcanonical rate constants were calculated for the five elementary steps involved in the CO and CO₂ elimination. The same equations



could be written down starting from the cis' and trans' isomers (the prime indicates cis or trans isomers after hydrogen migration between both oxygen atoms). This scheme leads to the following four kinetic equations:

$$\begin{pmatrix} d[\text{cis}]/dt \\ d[\text{trans}]/dt \\ d[\text{trans}']/dt \\ d[\text{cis}']/dt \end{pmatrix} = \begin{pmatrix} -k_{\text{CO}_2} - k_{\text{ct}} & k_{\text{tc}} & 0 & 0 \\ k_{\text{ct}} & -k_{\text{CO}_2} - k_{\text{ct}} - k_{\text{H}} & k_{\text{H}} & 0 \\ 0 & k_{\text{H}} & -k_{\text{CO}_2} - k_{\text{tc}} - k_{\text{H}} & k_{\text{ct}} \\ 0 & 0 & k_{\text{tc}} & -k_{\text{CO}_2} - k_{\text{ct}} \end{pmatrix} \begin{pmatrix} [\text{cis}] \\ [\text{trans}] \\ [\text{trans}'] \\ [\text{cis}'] \end{pmatrix}$$

The solutions of this system of differential equations were then used to get the concentrations of CO and CO₂ formed at $t \rightarrow \infty$. The microcanonical rate constants for the five elementary steps were calculated using the following RRKM expression:

$$k(E) = \sigma \frac{\sum_n P(E - \epsilon_n^{\text{ts}})}{h\rho(E)}$$

which includes tunneling corrections to the rate constants. In the above expression σ is the reaction path degeneracy, $P(E)$ is the one-dimensional tunneling probability as a function of energy E in the reaction coordinate and ϵ_n^{ts} are the vibrational levels of the transition state. Finally, $\rho(E)$ is the reactant density of states. At 248 nm, the tunneling corrections do not change the CO/CO₂ branching ratio significantly (~1%).

C. Classical Trajectory Calculations. The potential energy surface employed in the trajectory calculations was obtained by interpolation of 7042 energies, gradients, and Hessians at the B3LYP/aug-cc-pVDZ level, following the technique of Collins and co-workers as implemented in the Grow package.⁷ 5000 points were selected by starting the trajectories from either the cis and trans isomers after the CO/CO₂ branching ratio had converged, and the remaining 2042 points were selected starting the trajectories from the transition states associated to the CO and CO₂ elimination channels and propelling them toward the products.

Initial conditions were selected in three ways: (1) microcanonical (i.e., random) distribution of vibrational states at the trans-FA phase space (in the ground state), (2) the same type of distribution for cis-FA, and (3) a selective excitation of vibrational modes (preferentially the CH out-of-plane wagging and the C=O stretching) that mimics the conditions originated by the internal conversion process. To get this initial distribution after internal conversion, we calculated the optical oscillator strength arising from the vertical (i.e., Franck-Condon) transition and the contributions from each normal mode due to

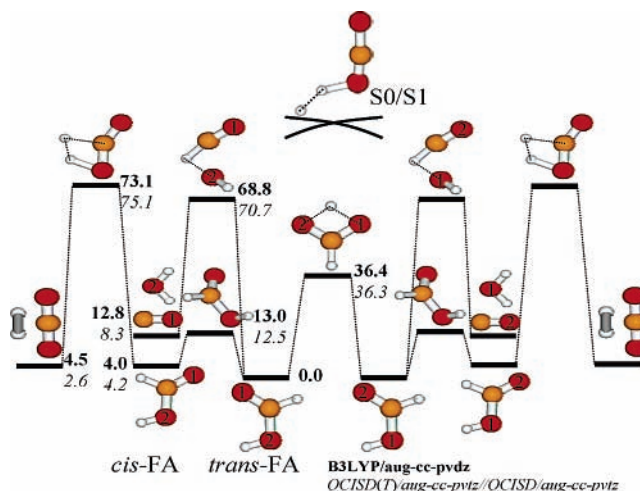


Figure 1. Relevant structures and energy profiles involving dissociation of FA in the ground state. Energies (without zero-point energy corrections) are in kcal/mol. A S₀/S₁ CI is also shown (see text).

vibronic coupling.⁸ The ground-state normal-mode frequencies computed at the MP2/cc-pVTZ level were scaled by 0.950, while to calculate the oscillator strengths we used state-averaged CASSCF(10,8)/cc-pVTZ electronic wave functions. Using a closure relation for the S₁ vibrational states and harmonic functions, we could integrate the calculated electronic transition dipole moments and obtain the corresponding optical oscillator strengths between the two states along each normal mode.

For each set of initial conditions, we employed batches of 5000 trajectories, which were integrated using the velocity Verlet algorithm with a step size of 0.005 fs.

Results and Discussion

Figure 1 shows the potential energy diagram for the lowest energy channels of FA (S₀) obtained at the QCISD(T)/aug-cc-pVTZ//QCISD/aug-cc-pVTZ level of theory. Our results show, in agreement with previous theoretical studies,^{4,5} that the transition state leading to CO + H₂O is about 4 kcal/mol lower in energy than that associated with CO₂ + H₂ formation. With respect to the study of Goddard et al.,⁴ we include here an additional channel connecting two trans-FA isomers via hydrogen migration (shown in the middle of Figure 1). By contrast, we did not include the high energy 1,2-hydrogen shift process leading to dihydroxymethylene, which is predicted to be about 10 kcal/mol higher in energy than the highest transition state of those considered here.⁴ For the dynamics study we employed cheaper B3LYP/aug-cc-pVDZ calculations,⁶ which as seen in Figure 1 compare reasonably well with our QCISD(T) results.

We carried out statistical RRKM and classical trajectory calculations to evaluate the CO/CO₂ ratios. The CO/CO₂ branching ratios obtained in this work for the photodissociation of FA at 248 nm are shown graphically in Figure 2. As can be seen, the results indicate that: (1) the dynamics for CO and CO₂ elimination is essentially statistical since the RRKM and trajectory branching ratios are rather similar to each other and the calculated ratio does not vary significantly with the location of the initial excitation within the molecule; (2) formation of CO + H₂O is the main channel; (3) the theoretical CO/CO₂ ratios (9–13) are in good agreement with that estimated from experiment (~11);^{1,9} and (4) formation of about 1/3 of the CO product involved a 1,3-H shift (see Figure 1). Our results, therefore, strongly suggest that the photodissociation of FA at 248 nm does not show substantial conformational memory, because the branching ratios obtained for dissociation from cis-FA and

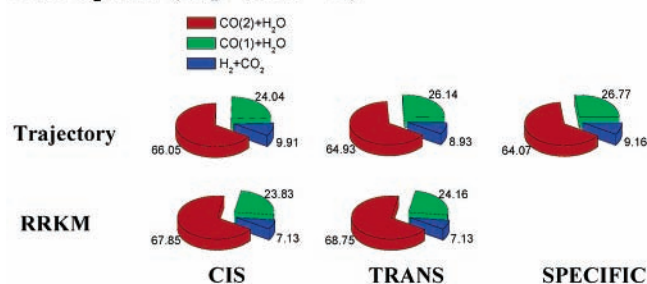
CO/CO₂ ratio (Exp¹ value ≈ 11)

Figure 2. Branching ratios obtained in the 248 nm photodissociation of FA.

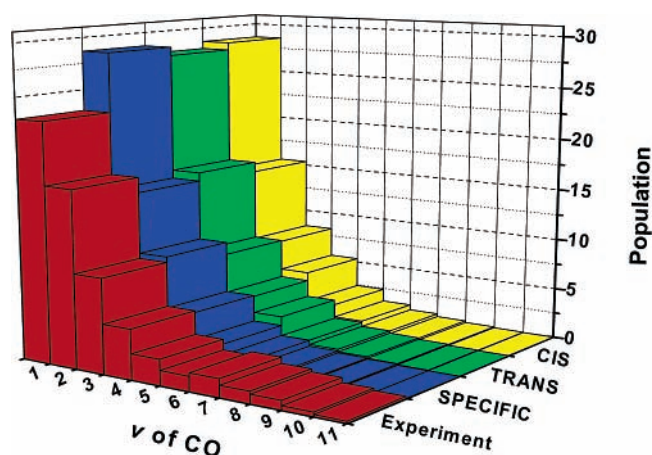


Figure 3. Comparison of relative vibrational distributions of CO after photodissociation of FA at 248 nm. Experimental data from ref 1.

from *trans*-FA are quite similar to each other. The CO + H₂O elimination dominates over CO₂ + H₂ because the former is energetically favored (by ~4 kcal/mol).

To check the reliability of our trajectory calculations, we compared in Figure 3 the CO vibrational distributions obtained by the trajectory calculations with those determined by Su et al.¹ As seen in the figure, the agreement with experiment is reasonably good. The fact that the experimental distribution is a bit hotter than the theoretical distribution may be explained by the lower reverse barrier height obtained by B3LYP (56.0 kcal/mol) compared with that predicted by the more accurate QCISD(T) computations (62.4 kcal/mol). Very recently, Kurosaki et al.¹⁰ computed the product energy distributions for the CO and CO₂ elimination channels by means of MP2/cc-pVDZ direct trajectories. Their computed CO vibrational distributions are in worse agreement with experiment than are ours. In particular, they did not find CO products with $v \geq 6$. They also predicted that the relative translational energy of the products for the CO₂ elimination channel (69.6 kcal/mol) is higher than that obtained for the CO elimination channel (37.2 kcal/mol). These values are in line with those obtained in the present work (51.6 and 30.5 kcal/mol, respectively). They claimed that the geometries of the involved transition states are responsible for the difference between the average values. In addition, the fact that the reverse barrier height for the CO₂ elimination is 13 kcal/mol higher than that for the CO elimination has some influence in the results.

Assuming that at 193 nm the formation of CO and CO₂ occurs entirely from the vibrationally excited ground state of FA, we performed trajectory calculations and obtained CO/CO₂ ratios of 5.0 and 5.8 for the initializations at *cis*-FA and *trans*-FA, respectively. Clearly, our results are not consistent with the proposed model of conformational memory.² It can be argued

that the Ar environment may play a significant role in the dissociation dynamics of FA. Petterson et al.¹¹ estimated the influence of the Ar matrix on the *trans*-to-*cis* barrier height using a polarizable continuum model and found that the barrier decreased by 111 cm⁻¹ with respect to that in the gas phase. Our B3LYP/6-31G* calculations on a FA molecule trapped in a cage of 12 Ar atoms (the coordination index for a cubic close-packed structure) also point out that the isomerization barrier does not vary significantly with respect to the gas-phase value. However, Lundell et al.¹² have found experimentally that the CO/CO₂ ratio is strongly dependent on the matrix material. In particular, they found that the CO₂ elimination channel is activated in a Xe matrix. Assuming that the solid Ar environment does not affect significantly the dynamics on the ground state, our results are at odds with the data and mechanism reported by Khriachtchev et al.² We suggest that the difference in the CO/CO₂ ratios found in the 193 nm photolysis of *cis*- and *trans*-FA² arises from subtle mechanisms on the S₁ excited state (and perhaps from the matrix environment), a reason not completely excluded by Khriachtchev et al.² An experimental study of the photodissociation of *cis*- and *trans*-FA in solid Ar at a lower wavelength (e.g., 248 nm) would provide additional insight into the dissociation mechanism in the ground state. Actually, Khriachtchev et al.² studied the photolysis of *trans*-FA at 234 nm in Ar matrix but, unfortunately, their equipment did not allow them to irradiate *cis*-FA at 234 nm. On the theoretical side, it would be desirable to explore the S₁ surface further and, even better, to carry out nonadiabatic dynamics calculations involving the S₁ and S₀ surfaces, too. For example, by state-averaged CASSCF(10,8)/cc-pVTZ calculations, we found a S₁/S₀ conical intersection (shown in Figure 1), with an energy similar to that of a different CI found by He and Fang,³ which would drive FA to CO₂ + H₂. Park et al.¹³ have recently found that different isomers of 1-iodopropane ions give rise to different products. Specifically, *gauche*-1-iodopropane ions produce 2-propyl ions while *anti*-1-iodopropane ions form protonated cyclopropane ions. In their study¹³ they excluded a mechanism in which, after internal conversion, the 1-iodopropane ions dissociate in the ground state, since “this would yield C₃H₇I⁺ species with a large amount of internal energy, and thus able to rapidly interconvert between the two different conformational states”. Therefore, this experimental work supports our present conclusion that the conformational memory observed by Su et al.¹ Khriachtchev et al.² cannot be explained by the dynamics on the ground state and that either the matrix material or the dynamics on the S₁ state or both are responsible for the results obtained in ref 2.

Acknowledgment. E.M.-N. and J.F.C. thank the Spanish Ministry of Science and Technology for their Ramón y Cajal research contracts. I.B.J. thanks Faperj and CNPq.

References and Notes

- (1) Su, H.; He, Y.; Kong, F.; Fang, W.; Liu, R. *J. Chem. Phys.* **2000**, *113*, 1891–1897.
- (2) Khriachtchev, L.; Maçôas, E.; Petterson, M.; Räsänen, M. *J. Am. Chem. Soc.* **2002**, *124*, 10994–10995.
- (3) He, H.-Y.; Fang, W.-H. *J. Am. Chem. Soc.* **2003**, *125*, 16139–16147.
- (4) Goddard, J. D.; Yamaguchi, Y.; Schaefer, H. F., III *J. Chem. Phys.* **1992**, *96*, 1158–1166.
- (5) Anglada, J. M.; Crehuet, R.; Bofia, J. M. *Chem. Eur. J.* **1999**, *5*, 1809–1821.
- (6) The B3LYP/aug-cc-pvdz level of theory was chosen for its better performance over B3LYP/6-311G(d,p), MP2/6-311G(d,p), MP2/aug-cc-pVDZ, and QCISD/aug-cc-pVDZ calculations.

(7) Jordan, M. J. T.; Thompson, K. C.; Collins, M. A. *J. Chem. Phys.* **1995**, *102*, 5647–5657. Thompson, K. C.; Jordan, M. J. T.; Collins, M. A. *J. Chem. Phys.* **1998**, *108*, 8302–8316. Bettens, R. P. A.; Collins, M. A. *J. Chem. Phys.* **1999**, *111*, 816–826.

(8) Borges, I., Jr.; Varandas, A. J. C.; Rocha, A. B.; Bielschowsky, C. E. *J. Mol. Struct. (THEOCHEM)* **2003**, *621*, 99–105 and references therein.

(9) The experimental ratio reported by Su et al.¹ is 7.5 and corresponds to $\text{CO}(v \geq 1)/\text{CO}_2(v \geq 1)$. However, the contribution from $\text{CO}(v = 0)$ is

substantial [not for $\text{CO}_2(v = 0)$]. Adding the $\text{CO}(v = 0)$ population predicted in this study, we obtained a ratio of ~ 11 .

(10) Kurosaki, Y.; Yokoyama, K.; Teranishi, Y. *Chem. Phys.* **2005**, *308*, 325–334.

(11) Petterson, M.; Maçôas, E. M. S.; Khriachtchev, L.; Fausto, R.; Räsänen, M. *J. Am. Chem. Soc.* **2003**, *125*, 4058–4059.

(12) Lundell, J.; Räsänen, M. *J. Mol. Struct.* **1997**, *436*, 349–358.

(13) Park, S. T.; Kim, S. K.; Kim, M. S. *Nature* **2002**, *415*, 306–308.